Hot Carrier-Induced Tautomerization within a Single Porphycene Molecule on Cu(111)

Janina N. Ladenthin,[†] Leonhard Grill,[†,‡] Sylwester Gawinkowski,[§] Shuyi Liu,[†] Jacek Waluk,[§] and Takashi Kumagai*[,†]

[†]Department of Physical Chemistry, Fritz-Haber Institute of the Max-Planck Society, Faradayweg 4-6, 14195 Berlin, Germany, [‡]Department of Physical Chemistry, University of Graz, Heinrichstrasse 28, 8010 Graz, Austria, and [§]Institute of Physical Chemistry, Polish Academy of Sciences, Kasprzaka 44/52, Warsaw 01-224, Poland

ABSTRACT Here, we report the study of tautomerization within a single porphycene molecule adsorbed on a Cu(111) surface using low-temperature scanning tunneling microscopy (STM) at 5 K. While molecules are adsorbed on the surface exclusively in the thermodynamically stable *trans* tautomer after deposition, a voltage pulse from the STM can induce the unidirectional *trans* → *cis* and reversible *cis* ↔ *cis* tautomerization. From the voltage and current dependence of the tautomerization yield (rate), it is revealed that the process is induced by vibrational excitation *via* inelastic electron tunneling. However, the metastable *cis* molecules are thermally switched back to the *trans* tautomer by heating the surface up to 30 K. Furthermore, we have found that the unidirectional tautomerization can be remotely controlled at a distance from the STM tip. By analyzing the nonlocal process in dependence on various experimental parameters, a hot carrier-mediated mechanism is identified, in which hot electrons (holes) generated by the STM travel along the surface and induce the tautomerization through inelastic scattering with a molecule. The bias voltage and coverage dependent rate of the nonlocal tautomerization clearly show a significant contribution of the Cu(111) surface state to the hot carrier-induced process.

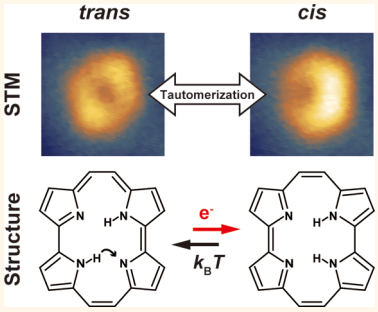

KEYWORDS: tautomerization · single molecule · scanning tunneling microscopy · metal surface · nonlocal adsorbate reaction · hot carrier transport

Intramolecular H atom transfer (tautomerization) is an important process in chemistry and biology[1] and is a long-standing research topic in organic chemistry (*e.g.*, as reported in the pioneering study by Claisen in 1896[2]). Tautomerization can modify molecular properties through a change of structural skeletons and electronic density distributions, which is directly related with chromism.[3] Recently, single molecule tautomerization has gained more attention in nanoscale science and technology since it resembles a molecular switch. For such applications, it is of fundamental importance to understand the tautomerization mechanism at the molecular level because impact from local surroundings on the process becomes much more significant at the nanometer scale.[4]

Recently, scanning tunneling microscopy (STM) has been used to investigate single molecule tautomerization within free-base phthalocyanine,[5] naphthalocyanine,[6] and porphyrin[7] at cryogenic temperature. In these experiments, tautomerization has been induced by the injection of tunneling electrons and inelastic electron tunneling was proposed as a possible mechanism. We have studied tautomerization within a single porphycene molecule and identified a vibrationally induced mechanism on a Cu(110) surface.[8] Additionally, the tautomerization behavior has been controlled by modifying the local surroundings of a molecule by using atom/molecule manipulation with an STM.[4] Adsorbate reactions can be induced by the STM not only directly under the tip, but also at lateral distances from it (up to ~100 nm in an extreme case),[6,9−16] allowing remote control of adsorbate reactions. For such *nonlocal* reactions, the transport of hot carriers or the effect of an electric field has been proposed as a possible mechanism. The two different origins were examined based on a distinct decay behavior of the tunneling electron and electric field.[12] The hot carrier mechanism has been identified on metal

* Address correspondence to kuma@fhi-berlin.mpg.de.

Received for review April 10, 2015 and accepted June 9, 2015.

Published online June 09, 2015
10.1021/acsnano.5b02147

surfaces,[11,14] wherein the hot electrons (holes) generated under the STM tip are expected to travel through surface states. However, the details of the transport mechanism are still unclear.

Porphycene is a structural isomer of porphine (free-base porphyrin).[17] They have comparable chemical properties, although the inner cavity geometry of porphycene is different. Therefore, in theory, a porphycene molecule can have three distinct tautomers with the different positions of the inner H atoms (see Supporting Information, Figure S1). Calculations have predicted that the *trans* configuration is most stable in the gas phase.[4,18] However, the tautomeric state and dynamics upon adsorption on surfaces is largely determined by the molecule−surface interaction, thus by the surface employed. For example, a porphycene molecule is found only as the *cis* tautomer on a Cu(110) surface and the reversible *cis* ↔ *cis* tautomerization can be induced by the STM-excitation.[4,8] Here, we study the role of the surface by using a Cu(111) surface that is selected for examining the different adsorption and tautomerization behaviors.

RESULTS AND DISCUSSION

Porphycene molecules on a Cu(111) surface are exclusively found in the *trans* tautomer on the terrace after deposition, and they adsorb as isolated monomers without aggregating into clusters or islands at the low coverage, similar to porphine molecules adsorbed on a Ag(111) surface.[19] Figure 1a shows typical STM images of *trans* molecules observed at 5 K. The symmetric appearance is consistent with the *trans* tautomer in which the H atoms in the molecular cavity are located on opposite pyrrole rings; this agrees with the simulated STM image on Cu(110).[4] The *trans* molecule shows six orientations, reflecting the 3-fold symmetry of the Cu(111) surface in combination with the mirror-symmetric configuration of the inner H atoms.

A porphycene molecule is stationary at relatively low bias voltages (<150 mV), while it can be converted to the *cis* tautomer at higher voltages. In Figure 1a,b a voltage pulse of −280 mV was applied for 100 ms over the upper molecule, and then it changed into the *cis* tautomer. The asymmetric appearance is consistent with the arrangement of the H atoms in the cavity, and the identical appearance is observed for the *cis* tautomer on Cu(110).[4,8] When we compare the molecular appearance with the surface crystallographic directions, it becomes clear that the long axis of a *cis* tautomer aligns along the high-symmetry axis of the surface (indicated by the three white lines next to the molecule in Figure 1b). In Figure 1b,c, the bottom *trans* molecule is converted to a differently oriented *cis* tautomer from Figure 1b (six different orientations exist because of the same reason with the *trans* tautomer as described above). Additionally, the reversible *cis* ↔ *cis* tautomerization can also be induced by a

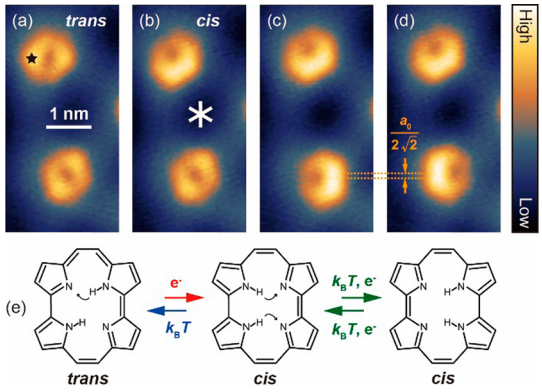

Figure 1. (a) Typical STM images of *trans* molecules at 5 K (I_t = 100 pA and V_s = −100 mV, image size: 5 × 2.5 nm^2, the color scale ranges from −15 to 82 pm). A voltage pulse of −280 mV is applied for 100 ms over the upper molecule while fixing the STM tip at the position indicated by the black star and at gap conditions of I_t = 100 pA and V_s = −100 mV. (b) After the pulse, the former *trans* molecule changes into a *cis* tautomer. The three white lines next to the molecule represent the high-symmetry axis of the surface. (c) The bottom molecule is converted to a *cis* tautomer. (d) *cis* ↔ *cis* tautomerization is induced in the bottom molecule. The molecule slightly migrates along the surface crystallographic direction approximately by ∼1.4 Å (≈ $a_0/2\sqrt{2}$). (e) Chemical structure of the *trans* and *cis* tautomer of a porphycene molecule can be selectively converted on a Cu(111) surface by STM- (e^-) or by thermal (k_BT) excitation. The H atom transfer is indicated by the arrows.

voltage pulse of the STM. In Figure 1c,d, the bottom *cis* molecule is switched to the mirror symmetric state. Note that the *cis* ↔ *cis* tautomerization involves a slight migration of a molecule approximately by ∼1.4 Å (≈$a_0/2\sqrt{2}$) along the surface crystallographic direction.

The STM-induced tautomerization shows a clear threshold voltage. Figure 2a displays the voltage dependence of the *trans* → *cis* and *cis* ↔ *cis* tautomerization yields. The tautomerization was induced while fixing the STM tip at the position indicated in the inset image (marked by the black stars), and a switching event was monitored by recording tunneling currents during voltage pulses. The yields exhibit an identical behavior for both bias polarities, and a threshold approximately at ±150 mV is found for both processes. Figure 2b shows the current dependence of the tautomerization yields measured at a bias voltage of ±250 and −170 mV for the *trans* → *cis* and *cis* ↔ *cis* tautomerization, respectively. The yields are independent of the tunneling current; thus, the process occurs *via* a one-electron process. These results clearly indicate that tautomerization is induced by vibrational excitation through an inelastic electron tunneling process. In contrast, the electronic excitation is unlikely because the HOMO−LUMO gap of porphycene is approximately 2.2 eV (for Q-band: $S_1 \leftarrow S_0$).[20] The active vibrational mode could be assigned to an in-plane mode of porphycene.[8]

Importantly, all *cis* molecules can be switched back to the *trans* tautomer by heating the surface up to

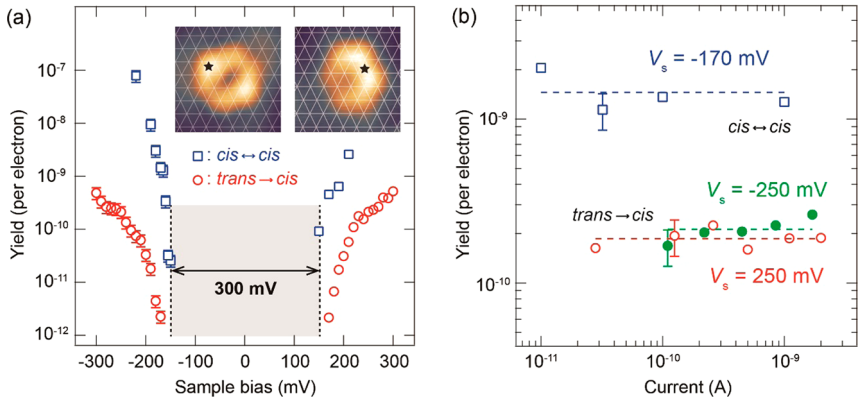

Figure 2. (a) Voltage dependence of the *trans* → *cis* (red circles) and *cis* ↔ *cis* (blue squares) tautomerization yields. The STM tip was fixed at the position indicated by the black stars in the inset images during the measurements. The white grid lines in the inset images represent the surface lattice of Cu(111). (b) Current dependence of the *trans* → *cis* (red and green circles) and *cis* ↔ *cis* (blue squares) tautomerization yields obtained at a bias voltage of ±250 and −170 mV, respectively.

~30 K, clearly indicating that the *trans* tautomer is more thermodynamically stable. Thermally induced *cis* ↔ *cis* tautomerization can also be observed in the range from 22 to 25 K. From the temperature-dependent tautomerization rate (and the corresponding Arrhenius plot, see Supporting Information, Figure S2), the barriers of the *cis* → *trans* and *cis* ↔ *cis* tautomerization are determined as 42.3(±2.7) and 34.6(±9.4) meV, respectively; thus, the former one appears to be little higher (because of the limited measurable temperature range, the error in the latter process becomes larger). On the other hand, we could not observe thermally induced the *trans* → *cis* tautomerization. This is because the *cis* tautomer is immediately switched back to *trans* at elevated temperatures, and the time-resolution of the STM (a few hundred microseconds) is not enough to capture the short-lived *cis* state. Figure 1e summarizes the tautomerization behavior of porphycene on a Cu(111) surface.

Interestingly, the *cis* → *trans* tautomerization could not be induced by the STM-excitation. The reason remains unclear, and even if the barrier of the *cis* ↔ *cis* tautomerization was slightly lower than that of *cis* → *trans*, it cannot be immediately rationalized because the threshold voltage (~150 mV, see Figure 2a) is much higher than the thermal barrier of both processes (~35 meV, *cis* ↔ *cis*; ~42 meV, *cis* → *trans*). Vibrationally induced reactions *via* inelastic electron tunneling differ from thermal processes, and it is not straightforward to compare them. The higher threshold voltage of the *cis* ↔ *cis* tautomerization compared to the thermal activation barrier implies that a higher frequency mode is associated with the tautomerization coordinate through anharmonic coupling. Such intermode coupling between an excited vibration mode and a reaction coordinate often plays a decisive role in the vibrationally induced process.[21] Therefore, for a complete understanding of the STM-induce tautomerization mechanism, it is necessary to clarify the vibration mode excited *via* inelastic electron tunneling (*i.e.*, the details of electron−phonon coupling) as well as multidimensional potential energy surfaces (including anharmonicity), which requires sophisticated density functional theory calculations combined with nonequilibrium theory and direct observation of the transition pathway of the tautomerization.

Thus far, we only discussed tautomerization directly under the STM tip during a voltage pulse. However, the process can also be induced in a *nonlocal* fashion, and molecules located far from the tip position (*i.e.*, the injection point of tunneling electrons) can be converted. In Figure 3a,b, a voltage pulse of −1.5 V for 50 ms was applied at the center of the image (indicated by the white star) while the feedback loop of the STM was disabled during the pulse (the tip−surface distance was fixed at gap conditions of $V_s = -50$ mV, and $I_t = 100$ pA). After the pulse, several molecules were switched to the *cis* tautomer (marked by the white circles in Figure 3b). Note that the nonlocal *cis* ↔ *cis* tautomerization can also be induced, but we focus on the unidirectional *trans* → *cis* process in the following.

Figure 3c shows the radial distance dependence of the *trans* → *cis* tautomerization rate measured with a voltage pulse of ±1.5 V (the vertical axis represents the ratio between the *cis* and *trans* molecules, see the figure caption). For a statistical analysis, we repeated the same measurement 14 (4) times, and counted ~10 000 (3000) molecules in total for voltage pulses of −1.5 (1.5) V. The radial distribution of the rate (Figure 3c) decays exponentially and exhibits a clear difference between the positive and negative bias. When fitting these data with an exponential decay function $e^{-r/\lambda}$, where λ is the decay constant and r is the lateral distance from the tip position, we obtain a good agreement and values of $\lambda \sim 13.5$ (6.4) nm for 1.5 (−1.5) V (the fitting was implemented at $r > 12.5$ nm for the 1.5 V pulse because of the saturation at the shorter radii).

STM-induced nonlocal adsorbate reactions have been reported on metal[9−14] and semiconductor[15,16]

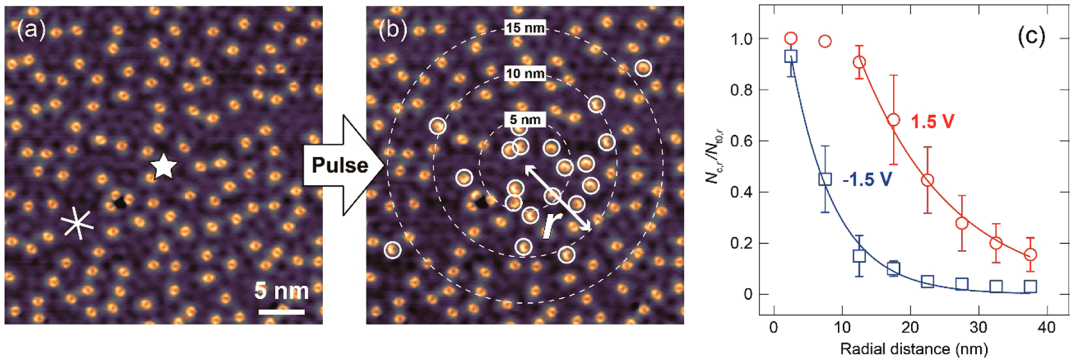

Figure 3. (a) Large-scale STM image of porphycene molecules on a Cu(111) surface at 5 K. A voltage pulse of −1.5 V was applied for 50 ms at the center of the image (indicated by the white star). The feedback loop of the STM was disabled during the voltage pulse at gap conditions of V_s = −50 mV, and I_t = 100 pA. (b) After the pulse, several molecules adsorbed far from the pulse position were converted into the *cis* tautomer (marked by the white circles). The broken circles in the image indicate the radial distance (r) from the pulse position. (c) Radial distance distribution of the tautomerization rates measured at a bias voltage of 1.5 V (red circles) and −1.5 V (blue squares) for 50 ms and with the coverage of 0.15(±0.005) nm^{-2} and gap conditions of V_s = −50 mV, and I_t = 100 pA. The vertical axis represents the ratio of the *cis* molecules (the number of $N_{c,r}$) with respect to the initial *trans* molecules (the number of $N_{t0,r}$) within a specific ring area (Δr = 5 nm) from the pulse position. The solid lines represent the best fit using an exponential decay.

surfaces, and the process was attributed either to transport of a hot carrier[9,11,13,14] or to an electric field.[10,22−25] In the hot carrier mechanism, tunneling electrons (holes) injected from the STM tip generate hot carriers that travel along the surface and remotely trigger the reactions at a distance from the tip through an inelastic scattering event with a molecule. On the other hand, the electric field in the STM modifies a potential landscape of the reactions[26] and the magnitude would decay more slowly than the tunneling current.[12] To examine the major contribution in the present case, we investigated the nonlocal tautomerization behavior by using a monoatomic step on a Cu(111) surface. When a voltage pulse is applied at the lower terrace and very close to the step edge (Figure 4a), a higher electric field is expected on the upper terrace. On the other hand, hot carriers generated under the tip may be scattered at the step edge, giving rise to less number of carriers on the upper terrace than on the lower one. Figure 4b illustrates the experimental configuration. Figure 4c shows the tautomerization rate after a voltage pulse at the upper (green squares) and lower terrace (blue circles) obtained in a series of different experiments. The *trans* → *cis* tautomerization is induced on both terraces, but the rate is always higher at the lower terrace (see also the dependence on the radial distance in Supporting Information, Figure S3), suggesting that the hot carrier-mediated process plays a decisive role. We also examined the switching behavior using a conductive cluster on the surface, and no contributions from an electric field were observed (see Supporting Information, Figure S4). Another indication of a hot carrier-mediated process is the fact that the tautomerization rate decreases exponentially with increasing the tip−surface distance (Figure 4d), and the decay constant of ∼5 nm^{-1} is comparable with that of the tunneling

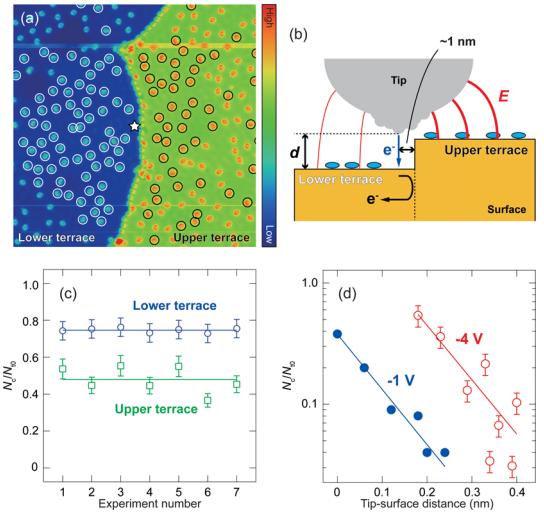

Figure 4. (a) Large-scale STM image of porphycene molecules on a Cu(111) surface with a monatomic step (V_s = −50 mV, I_t = 50 pA, image size: 45 × 45 nm^2, the color scale ranges from −0.01 to 0.37 nm). A voltage pulse of 1 V was applied for 1 s with I_t = 100 pA at a lateral distance of approximately 1 nm from the step edge. Switched (*cis*) molecules are indicated by the white (lower terrace) and black (upper terrace) circles. (b) Schematic of the experimental configuration in (a). (c) Tautomerization rate (N_c/N_{t0}) at the upper (green squares) and lower (blue circles) in the different measurements. (d) Tip−surface distance dependence of N_c/N_{t0} measured with a voltage pulse (50 ms duration) of −1 V (blue filled circles) and −4 V (red open circles) within an area of 50 × 50 nm^2. The zero-point in the horizontal axis corresponds to gap conditions of V_s = 50 mV and I_t = 3 nA. The solid lines represent the best fit with an exponential decay.

current (∼10 nm^{-1}).[27] The deviation may be attributed to the underestimation of the tautomerization rate at shorter distances because of the saturation in the central region. Furthermore, identical behaviors were observed in the nonlocal tautomerization even if we used different STM tips whose apex structure is considerably different from each other (see Supporting

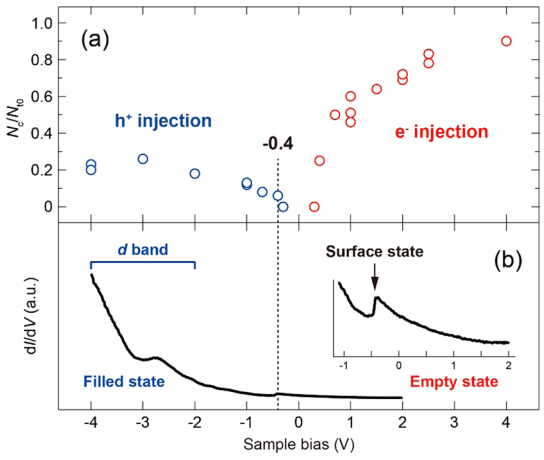

Figure 5. (a) Voltage dependence of the hot carrier-induced tautomerization rates measured at the coverage of 0.07(±0.005) nm^{-2}. The rate (N_c/N_{to}) was determined within the measurement area of 80 × 80 nm^2 after pulses at various voltages, with a constant current of 250 pA (corresponding to 1.56 × 10^9 electrons), were applied for 1 s. The positive and negative bias voltages correspond to the electron (e^-) and hole (h^+) injection into the surface, respectively. (b) STS spectra (d*I*/d*V*) measured over a bare Cu(111) surface. The stepwise feature due to the surface state is clearly observed approximately at −0.4 V, while relatively high DOS resulting from the Cu *d*-band is observed at the negative bias (filled states). The inset displays the magnified spectrum around the Cu(111) surface state.

Information, Figure S5), which is in contrast to what might be expected for an electric field induced process where the precise field depends on the tip shape.[28] From these results, we conclude that the nonlocal tautomerization is induced dominantly by the hot carrier mechanism rather than by the electric field in the junction.

Figure 5a shows the voltage dependence of the nonlocal *trans* → *cis* tautomerization rate. The positive and negative sample bias voltages correspond to an electron and a hole injection to the surface, respectively, and the rates are much higher at positive bias. The electronic states that transport the hot carriers remain obscure in the previous studies.[11,14] It has also been suggested that bulk states might contribute to the hot carrier transport[11] because they behave similar to surface states at the edge of the projected band gap.[29] Figure 5b shows the scanning tunneling spectroscopy (STS) data measured on a bare Cu(111) surface. The surface state existing above −0.4 V with respect to E_F[30] is clearly observed (see the inset of Figure 5b), while high density of states resulting from the Cu *d*-band appear in the regime of filled states.[31] However, no significant contribution from the *d*-band to the tautomerization rate (Figure 5a) is observed. These results suggest that the hot electrons can induce the nonlocal tautomerization *via* the surface state much more efficiently than hot holes.

The surface state is to be affected by the adsorption of molecules, and *vice versa*, and STM provides a unique opportunity to investigate such phenomena *locally*,[32,33] which can only partially be addressed with spatial averaging methods. Figure 6a shows the distribution of the nearest neighbor distance (d_{NN}) between molecules at various coverages. Figure 6b−e displays the corresponding STM images and the molecules remain isolated at these coverages. At coverages below approximately 0.1 nm^{-2}, the d_{NN} exhibits the first peak at 2.5(±0.1) nm and a characteristic oscillation at a distance of 1.3(±0.1) nm. This length coincides with half of the Fermi wavelength ($\lambda_F/2$) of the Cu(111) surface state (as is clearly observed at 0.03 nm^{-2}), indicating the long-range interactions between molecules mediated *via* the surface state.[34−37] The deviation from $\lambda_F/2$ at the first peak (∼2.5 nm) may be due to the finite size of a molecule (∼1 nm) and the scattering of the surface electrons occurs at the edge of the molecule. The oscillatory feature is still discernible at 0.06 nm^{-2}, but the separation deviates from 1.3 nm ($\lambda_F/2$). This is because the higher-order neighbor distances are not counted, which causes an apparent shift of the peak position resulting from the surface mediated intermolecular interaction at intermediate coverages. However, it can be observed between the first and second neighbor distributions in the whole pair distances analysis (see Supporting Information, Figure S6). In contrast, these features are absent at coverages above 0.1 nm^{-2} and the d_{NN} monotonically decreases (Figure 6f, left axis) since molecules are forced to adsorb at smaller distances. Additionally, the standing wave pattern of surface electrons is hidden underneath the molecules at higher coverages and cannot be resolved in the STM (see the inset images at the bottom of Figure 6a), and the surface state cannot be observed in STS measurements (as discussed in detail in Figure 7). These observations suggest that the molecules and surface are differently interact at low and high coverages. Figure 6f (right axis) also shows the *trans* → *cis* tautomerization yield of a single molecule measured with a bias voltage of −300 mV. Importantly, the yields do not change below and above a coverage of ∼0.1 nm^{-2}, indicating no significant impacts from the surface-mediated interaction on the tautomerization rate of individual molecules.

Next, to examine the influence from molecular coverage on the nonlocal tautomerization, we investigated the coverage-dependent behavior of the nonlocal process. Figure 6g displays the time-evolution of the nonlocal *trans* → *cis* tautomerization rate measured with a voltage pulse of 300 mV for four different coverages of 0.03(±0.005), 0.06(±0.005), 0.15(±0.005), and 0.33(±0.005) nm^{-2}. The saturation of the conversion rate indicates that the process has a finite effective range. The time-evolution series were also measured with different tip conditions (changed by gently

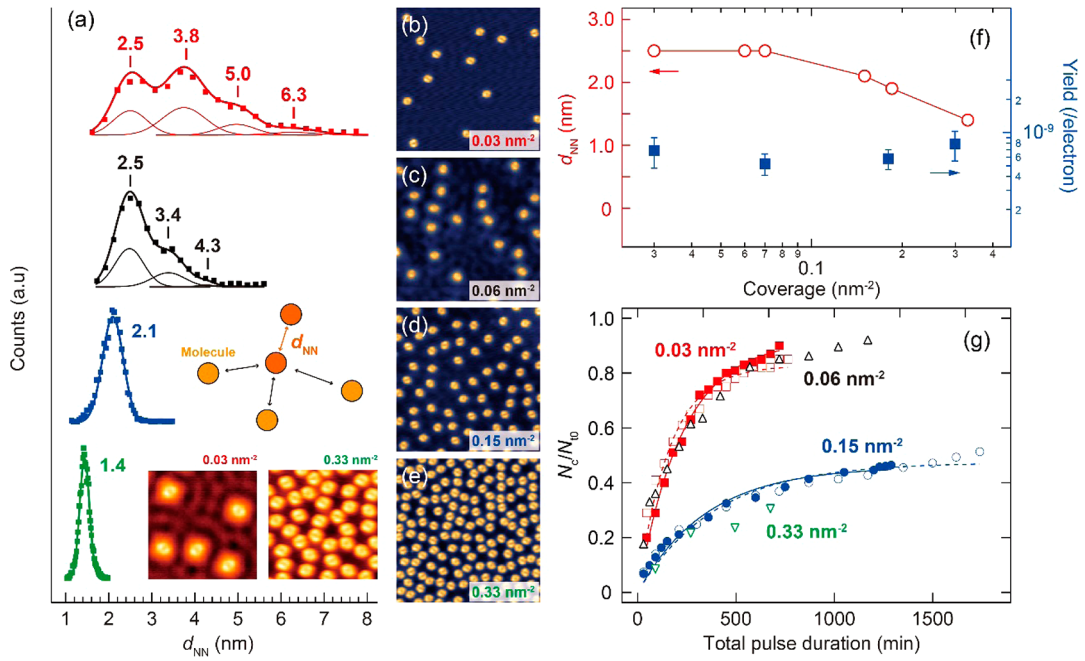

Figure 6. (a) Coverage dependent distribution of the nearest neighbor distances (d_{NN}) between molecules. More than 1300 molecule pairs were counted. The bottom inset displays enlarged and contrast-enhanced STM images (size: 10 × 10 nm^2) for a coverage of 0.03 and 0.33 nm^{-2}. (b–e) STM images (size: 20 × 20 nm^2) at a coverage of 0.03(±0.005) nm^{-2} (b), 0.06(±0.005) nm^{-2} (c), 0.15(±0.005) nm^{-2} (d), and 0.33(±0.005) nm^{-2} (e). (f) Coverage dependence of the first peak of d_{NN} (left axis) and *trans* → *cis* tautomerization yield (right axis) of individual molecules. The yield was measured with a voltage pulse of −300 mV. (g) Time-evolution of the nonlocal *trans* → *cis* tautomerization rate measured at a coverage of 0.03 nm^{-2} (red squares), 0.06 nm^{-2} (black triangles), 0.15 nm^{-2} (blue circles), and 0.33 nm^{-2} (green triangles). The open and filled squares (circles) for 0.03 (0.15) nm^{-2} were obtained with different tip conditions. The vertical axis represents the ratio of the total number of *cis* (N_c) to the initial number of *trans* (N_{t0}) molecules within the measurement area of 70 × 70 nm^2, and the voltage pulses of 300 mV were applied at the center of the measurement area while the tip was fixed at the gap conditions of V_s = −50 mV and I_t = 10 pA, resulting in the tunneling current of 0.07(±0.025) nA during the pulse. The solid (broken) curves represent the best fits using eq 2 for coverages of 0.03 and 0.15 nm^{-2}.

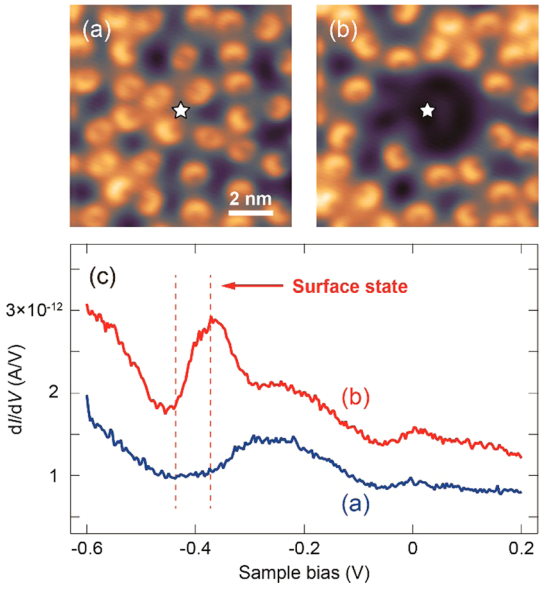

Figure 7. (a) STM image of porphycene molecules on a Cu(111) surface at a coverage of ~0.30 nm^{-2} (V_s = 50 mV, I_t = 50 pA, image size: 10 × 10 nm^2). (b) The same area as in (a) after removing the molecules by STM manipulating. (c) STS spectra measured over the bare Cu surface in (a) and (b) (the tip positions are indicated by white stars).

crashing the tip into the surface) for a coverage of 0.03 and 0.15 nm^{-2} (as indicated by the open and filled markers), but no significant differences were observed. Thus, tip effects can be excluded. Interestingly, the behavior is almost the same at 0.03 and 0.06 nm^{-2}, and at 0.15 and 0.33 nm^{-2}, respectively. A higher rate is observed at lower coverages where molecules interact *via* the surface state and are separated by the characteristic distance (determined by the Fermi wavelength). If scattering of the hot carriers with a molecule governed their decay, the rate should monotonically decrease with increasing molecular coverage, which is not the case. Thus, the above results (Figure 6g) indicate that the scattering is negligible in the transport efficiency and the decay of the hot carriers may be governed by electron–electron and electron–phonon scattering.

The nonlocal hot carrier process can be analyzed by using the following rate equation:[11]

$$\frac{dN_{c,r}}{dt} = k(N_{t0,r} - N_{c,r})I_r^n \qquad (1)$$

where $N_{c,r}$ ($N_{t0,r}$) is the (initial) number of the *cis* (*trans*) molecules at the radial distance r, I_r is the current (the number of the hot carriers) at r, and n is the reaction order. Note that eq 1 assumes a specific

effective area where the nonlocal reaction occurs. Equation 1 then gives

$$\frac{N_c}{N_{t0}} = N(\infty)(1 - e^{-kI_{eff}^n t}) \quad (2)$$

where N_c and N_{t0} are the (initial) number of *cis* (*trans*) molecules within the measured area, $N(\infty)$ the ratio of the *cis* to *trans* populations at $t = \infty$, and $I_{eff} = I_t \sum_r e^{-(r/\lambda)}$ represents the total number of the effective hot carriers associated with the nonlocal process. The time-evolution of N_c/N_{t0} in Figure 6g can be reproduced by eq 2, and here we assume $n = 1$ because a one-electron process is expected at the excitation voltage of 300 mV (see Figure 2b). The solid (dashed) lines in Figure 6g represent the best fit to the results, and $kI_{eff} \sim 8.8(\pm 2) \times 10^{-5}$ s^{-1} and $4.5(\pm 1) \times 10^{-5}$ s^{-1} is obtained for the coverage of 0.03 and 0.15 nm^{-2}, respectively.[38]

The above results clearly indicate that the Cu(111) surface state plays a crucial role in the nonlocal tautomerization process. The interesting observation is a noticeable difference in the rate between the low (0.03 and 0.06 nm^{-2}) and high (0.15 and 0.33 nm^{-2}) coverages (Figure 6g). This suggests that a critical modification of the surface state occurs at a coverage of ~0.1 nm^{-2}, which may affect the decay mechanism of hot carriers (*i.e.*, electron−electron and electron−phonon scattering). It has previously been found that adsorbates influence surface states, for instance, a continuous shift and attenuation of the surface state was revealed in adsorption of CO molecules on a Cu(111) surface by using photoelectron spectroscopy.[39] However, in contrast to porphycene molecules, CO forms molecular island even at low coverages because of the attractive intermolecular interaction,[40] presumably leading to a distinct influence on the surface state in contrast to our case (*i.e.*, the abrupt change at a specific coverage). We deduce that, at low coverages, the surface state is not strongly affected by molecular adsorption because the surface mediated interaction (as seen in Figure 6a) arranges porphycene molecules at "innocuous" sites to the surface state, while it may be ruptured rapidly above the critical coverage (~0.1 nm^{-2}). Such a demolition of the surface state was examined by using STS. Figure 7a shows an STM image at a coverage of ~0.30 nm^{-2}, and Figure 7b is the same area after removing molecules by STM manipulation. Figure 7c displays the STS spectra measured over the bare Cu area (the positon is indicated by the white stars) in Figure 7a (blue line) and b (red line), and the characteristic feature from the surface state around −0.4 V is absent in the former case, but can be recovered after sweeping the molecules. This result suggests that the surface state is quenched in the region where molecules are densely packed (*i.e.*, intermolecular spacing less than $\lambda_F/2$) and implies that the surface state can be *locally* engineered through molecule−surface interactions. However, further explanation of the hot carrier transport mechanism requires the elucidation of the transport channel and the variation of the band structure (dispersion relation).

CONCLUSIONS

In summary, tautomerization within a single porphycene molecule was studied on a Cu(111) surface using low-temperature STM. All molecules are adsorbed in the thermodynamically stable *trans* tautomer on the terrace after deposition. This is a critical difference from the adsorption on a Cu(110) surface and highlights the importance of molecule−surface interaction. The unidirectional *trans* → *cis* and reversible *cis* ↔ *cis* tautomerization can be induced by a voltage pulse from the STM. The voltage and current dependence of the tautomerization yield clearly indicate vibrationally induced process *via* inelastic electron tunneling. Metastable *cis* molecules can be thermally switched back to the *trans* tautomer by heating the surface up to 30 K. The thermal barriers of 42.3(±2.7) and 34.6(±9.4) meV were determined for the *trans* → *cis* and *cis* ↔ *cis* tautomerization, respectively, by measuring the temperature dependent tautomerization rates (Arrhenius plot). Furthermore, it was found that hot carriers generated in the surface by the STM can induce tautomerization in a nonlocal fashion. The voltage dependence of the nonlocal process showed that hot electrons are transported more efficiently through the Cu(111) surface state as compared to hot holes. Additionally, we revealed that the tautomerization rate of individual molecules is not affected by molecular coverage and the modification of the surface state has a crucial impact on the nonlocal process. These results demonstrate a remote control of molecular switching on a surface and provide microscopic insight into the processes.

METHODS

All experiments were performed in an ultrahigh vacuum chamber (base pressure of 10^{-10} mbar), equipped with a low-temperature STM (modified Omicron instrument with Nanonis Electronics). STM measurements were carried out at 5 K and the images were acquired in the constant-current mode. The bias voltage was applied to either the tip (V_t) or sample (V_s), and all voltages are shown as the sample bias V_s (= $-V_t$). The Cu(111) surface was cleaned by repeated cycles of argon ion sputtering and annealing to 700−800 K. The STM tip made from a W or PtIr wire was optimized *in situ* by applying a voltage pulse and poking it into the surface. Porphycene molecules were deposited from a Knudsen cell (at an evaporation temperature of 450−500 K). STS (d*I*/d*V*) spectra were recorded with a lock-in amplifier with a voltage modulation of 20−30 mV at 710 Hz frequency.

Conflict of Interest: The authors declare no competing financial interest.

Acknowledgment. The authors thank W. Frandsen and M. Willinger for contributions of SEM measurements. J.N.L, T.K., and L.G. thank M. Wolf for valuable discussions. T.K. acknowledges the support of Morino Foundation for Molecular Science. L.G. acknowledges financial support from the German Science Foundation (DFG) *via* the SFB project "Elementary Processes in Molecular Switches at Surfaces". S.G. and J.W. acknowledge the support by the Polish National Science Centre Grant DEC-2011/02/A/ST5/00043

Supporting Information Available: Tautomers of a porphycene molecule, temperature dependent tautomerization rate, radial distance dependence of nonlocal tautomerization rate at a step edge, nonlocal tautomerization induced through a conductive cluster on the surface, SEM images of the used STM tips prepared by different methods, intermolecular distance distribution analysis. The Supporting Information is available free of charge on the ACS Publications website at DOI: 10.1021/acsnano.5b02147.

REFERENCES AND NOTES

1. Antonov, L. *Tautomerism*; Wiley-VCH Verlag GmbH & Co.: Weinheim, Germany, 2014.
2. Claisen, L. Beiträge zur Kenntniss der 1,3-Diketone und verwandter Verbindungen. *Justus Liebigs Ann. Chem.* **1896**, *291*, 25–137.
3. Ohshima, A.; Momotake, A.; Arai, T. Photochromism, Thermochromism, and Solvatochromism of Naphthalene-Based Analogues of Salicylideneaniline in Solution. *J. Photochem. Photobiol., A* **2004**, *162*, 473–479.
4. Kumagai, T.; Hanke, F.; Gawinkowski, S.; Sharp, J.; Kotsis, K.; Waluk, J.; Perrson, M.; Grill, L. Controlling Intramolecular Hydrogen Transfer in a Porphycene Molecule with Single Atoms or Molecules Located Nearby. *Nat. Chem.* **2014**, *6*, 41–46.
5. Sperl, A.; Kröger, J.; Berndt, R. Controlled Metalation of a Single Adsorbed Phthalocyanine. *Angew. Chem., Int. Ed.* **2011**, *50*, 5294–5297.
6. Liljeroth, P.; Repp, J.; Meyer, G. Current-Induced Hydrogen Tautomerization and Conductance Switching of Naphthalocyanine Molecules. *Science* **2007**, *317*, 1203–1206.
7. Auwärter, W.; Seufert, K.; Bischoff, F.; Ecija, D.; Vijayaraghavan, S.; Joshi, S.; Klappenberger, F.; Samudrala, N.; Barth, J. V. A Surface-Anchored Molecular Four-Level Conductance Switch Based on Single Proton Transfer. *Nat. Nanotechnol.* **2012**, *7*, 41–46.
8. Kumagai, T.; Hanke, F.; Gawinkowski, S.; Sharp, J.; Kotsis, K.; Waluk, J.; Perrson, M.; Grill, L. Thermally and Vibrationally Induced Tautomerization of Single Porphycene Molecules on a Cu(110) Surface. *Phys. Rev. Lett.* **2013**, *111*, 246101.
9. Stipe, B. C.; Rezaei, M. A.; Ho, W. Atomistic Studies of O_2 Dissociation on Pt(111) Induced by Photons, Electrons, and by Heating. *J. Chem. Phys.* **1997**, *107*, 6443–6447.
10. Alemani, M.; Peters, M. V.; Hecht, S.; Rieder, K.-H.; Moresco, F.; Grill, L. Electric Field-Induced Isomerization of Azobenzene by STM. *J. Am. Chem. Soc.* **2006**, *128*, 14446–14447.
11. Maksymovych, P.; Dougherty, D. B.; Zhu, X.-Y.; Yates, T. Nonlocal Dissociative Chemistry of Adsorbed Molecules Induced by Localized Electron Injection into Metal Surfaces. *Phys. Rev. Lett.* **2007**, *99*, 016101.
12. Silien, C.; Liu, N.; Ho, W.; Maddox, J. B.; Mukamel, S.; Liu, B.; Bazan, G. C. Reversible Switching among Three Adsorbate Configurations in a Single [2.2]Paracyclophane-Based Molecule. *Nano Lett.* **2008**, *8*, 208–213.
13. Chen, L.; Li, H.; Wee, A. T. S. Nonlocal Chemical Reactivity at Organic-Metal Interfaces. *ACS Nano* **2009**, *3*, 3684–3690.
14. Hahn, J. R.; Jang, S. H.; Kim, K. W.; Son, S. B. Hot Carrier-Selective Chemical Reactions on Ag(110). *J. Chem. Phys.* **2013**, *139*, 074707.
15. Sloan, P. A.; Sakulsermsuk, S.; Palmer, R. E. Nonlocal Desorption of Chlorobenzene Molecules from the Si(111)−(7 × 7) Surface by Charge Injection from the Tip of a Scanning Tunneling Microscope: Remote Control of Atomic Manipulation. *Phys. Rev. Lett.* **2010**, *105*, 048301.
16. Bellec, A.; Rieded, D.; Dujardin, G.; Boudrioua, O.; Chaput, L.; Stauffer, L.; Sonnet, P. Nonlocal Activation of a Bistable Atom through a Surface State Charge-Transfer Process on Si(100)−(2 × 1):H. *Phys. Rev. Lett.* **2010**, *105*, 048302.
17. Vogel, E.; Köcher, M.; Schmickler, H.; Lex, J. Porphycene—A Novel Porphin Isomer. *Angew. Chem., Int. Ed. Engl.* **1986**, *25*, 257–259.
18. Wu, Y.-D.; Chan, K. W. K.; Yip, C.-P.; Vogel, E.; Plattner, D. A.; Houk, K. N. Porphyrin Isomers: Geometry, Tautomerism, Geometrical Isomerism, and Stability. *J. Org. Chem.* **1997**, *62*, 9240–9250.
19. Bischoff, F.; Seufert, K.; Auwäter, W.; Joshi, S.; Vijayaraghavan, S.; Ecija, D.; Diller, K.; Papageorgiou, A. C.; Fischer, S.; Allegretti, F.; et al. How Surface Bonding and Repulsive Interactions Cause Phase Transformations: Ordering of a Prototype Macrocyclic Compound on Ag(111). *ACS Nano* **2013**, *7*, 3139–3149.
20. Waluk, J.; Müller, M.; Swiderek, P.; Köcher, M.; Vogel, E.; Hohlneicher, G.; Michl, J. Electronic States of Porphycenes. *J. Am. Chem. Soc.* **1991**, *113*, 5511–5527.
21. Komeda, T.; Kim, Y.; Kawai, M.; Persson, B. N. J.; Ueba, H. Lateral Hopping of Molecules Induced by Excitation of Internal Vibration Mode. *Science* **2002**, *295*, 2055–2058.
22. Persson, B. N. J.; Avouris, P. The Effects of the Electric Field in the STM on Excitation Localization. Implications for Local Bond Breaking. *Chem. Phys. Lett.* **1995**, *242*, 483–489.
23. Avouris, Ph.; Walkup, R. E.; Rossi, A. R.; Akpati, H. C.; Nordlander, P.; Shen, T.-C.; Abeln, G. C.; Lyding, J. W. Breaking Individual Chemical Bonds *via* STM-Induced Excitations. *Surf. Sci.* **1996**, *363*, 368–377.
24. Cranney, M.; Mayne, A. J.; Laikhtman, A.; Comtet, G.; Dujardin, G. STM Excitation of Individual Biphenyl Molecules on Si(100) Surface: DIET or DIEF? *Surf. Sci.* **2005**, *593*, 139–146.
25. Rezaei, M. A.; Stipe, B. C.; Ho, W. Atomically Resolved Adsorption and Scanning Tunneling Microscope Induced Desorption on a Semiconductor: NO on Si(111)-(7 × 7). *J. Chem. Phys.* **1999**, *110*, 4891–4896.
26. Füchsel, G.; Klamroth, T.; Dokić, J.; Saalfrank, P. On the Electronic Structure of Neutral and Ionic Azobenzenes and Their Possible Roles as Surface Mounted Molecular Switches. *J. Phys. Chem. B* **2006**, *110*, 16337–16345.
27. Chen, C. J. *Introduction to Scanning Tunneling Microscopy*; 2nd ed.; Oxford University Press: Oxford, U.K., 2007; pp 3−5.
28. Feenstra, R. M. Electrostatic Potential for a Hyperbolic Probe Tip near a Semiconductor. *J. Vac. Sci. Technol., B* **2003**, *21*, 2080–2088.
29. Pascual, J. I.; Dick, A.; Hansmann, M.; Rust, H.-P.; Neugebauer, J.; Horn, K. Bulk Electronic Structure of Metals Resolved with Scanning Tunneling Microscopy. *Phys. Rev. Lett.* **2006**, *96*, 046801.
30. Gartland, P. O.; Slagsvold, B. J. Transitions Conserving Parallel Momentum in Photoemission from the (111) Face of Copper. *Phys. Rev. B* **1975**, *12*, 4047.
31. Knapp, J. A.; Himpsel, F. J.; Eastman, D. E. Experimental Energy Band Dispersions and Lifetimes for Valence and Conduction Bands of Copper using Angle-Resolved Photoemission. *Phys. Rev. B* **1979**, *19*, 4952.
32. Temirov, R.; Soubatch, S.; Luican, A.; Tautz, F. S. Free-Electron-like Dispersion in an Organic Monolayer Film on a Metal Substrate. *Nature* **2006**, *444*, 350–353.
33. Rojas, G.; Simpson, S.; Chen, X.; Kunkel, D. A.; Nitz, J.; Xiao, J.; Dowben, P. A.; Zurek, E.; Enders, A. Surface State Engineering of Molecule−Molecule Interactions. *Phys. Chem. Chem. Phys.* **2012**, *14*, 4971–4976.
34. Hyldgaard, P.; Persson, M. Long-Range Adsorbate−Adsorbate Interactions Mediated by a Surface-State Band. *J. Phys.: Condens. Matter* **2000**, *12*, L13–L19.
35. Repp, J.; Moresco, F.; Meyer, G.; Rieder, K.-H.; Hyldgaard, P.; Persson, M. Substrate Mediated Long-Range Oscillatory Interaction between Adatoms: Cu/Cu(111). *Phys. Rev. Lett.* **2000**, *85*, 2981–2984.
36. Knorr, N.; Brune, H.; Epple, M.; Hirstein, A.; Scheider, M. A.; Kern, K. Long-Range Adsorbate Interactions Mediated by a

Two-Dimensional Electron Gas. *Phys. Rev. B* **2002**, *65*, 115420.
37. Yokoyama, T.; Takahashi, T.; Shinozaki, K.; Okamoto, M. Quantitative Analysis of Long-Range Interactions between Adsorbed Dipolar Molecules on Cu(111). *Phys. Rev. Lett.* **2007**, *98*, 206102.
38. Given $k \sim 5 \times 10^{-10}$ (referring to the yield at $V_s = 300$ mV in Figure 2a), $I_{eff} \sim 0.028$ and 0.014 pA is estimated for a coverage of 0.03 and 0.15 nm^{-2}, respectively, which correspond to only a tiny fraction (<0.04%) of the injected tunneling current (0.07 nA).
39. Lindgren, S. Å.; Paul, J.; Walldén, L. Surface State Energy Shifts by Molecular Adsorption: CO on Clean and Na Covered Cu(111). *Surf. Sci.* **1982**, *117*, 426–433.
40. Bartels, L.; Meyer, G.; Rieder, K.-H. The Evolution of CO Adsorption on Cu(111) as Studied with Bare and CO-Functionalized Scanning Tunneling Tips. *Surf. Sci.* **1999**, *432*, L621–L626.